CHAPTER 2

Hydrothermally-Stable Alumina-Silica Composite Membranes for Hydrogen Separation

2.1. Introduction

This chapter describes in detail the preparation of hydrothermally-stable silica based membranes. A thin layer of a dual-element alumina-silica composition was deposited on a porous alumina support by chemical vapor deposition (CVD) in an inert atmosphere at high temperature. Prior to CVD, multiple graded layers of alumina were coated on the macroporous alumina support. The resulting supported composite membrane exhibited excellent stability to water vapor at high temperatures, while retaining high permeability for hydrogen in the order of 10^{-7} mol m^{-2} s^{-1} Pa^{-1} at 873 K with selectivities of H_2 over CH_4, CO and CO_2 of 940, 700 and 590, respectively.

2.2. Experimental

The alumina-silica composite membranes were deposited on macroporous alumina supports by a chemical vapor deposition (CVD) technique. Prior to deposition of the alumina-silica composite top layer, an intermediate γ-alumina multilayer with a graded structure was placed on the support. The intermediate γ-alumina layer was prepared by a dip-coating method

with a series of dilute dipping solutions containing boehmite sols of different particle sizes to form a graded structure.

2.2.1. Preparation of boehmite sols

Three boehmite (AlOOH) sols with a median particle size of 40, 200 and 630 nm (denoted as BS40, BS200 and BS630, respectively) were prepared by carefully controlling the hydrolysis of aluminum alkoxides and the subsequent acid peptization of the boehmite precipitate obtained, as reported elsewhere [1]. Table 2.1 lists the synthesis parameters of these boehmite sols. The general procedure for preparing the boehmite sols was as follows. A quantity of 0.2 mol of aluminum isopropoxide (Aldrich, 98+ %) was added to 300 ml of distilled water at room temperature. The mixture was quickly heated to 353 K within 0.5 h with high speed stirring and was maintained at this temperature for 3-24 h for the hydrolysis of the isopropoxide. The resulting boehmite precipitate was then heated to 365 K and was peptized using a quantity of acetic acid (GR, 99.7%) with a molar ratio of H^+/Alkoxide in the range of 0.04-0.15. The solution was refluxed at 365 K for 20 h to get a clear or slightly translucent sol.

Table 2.1. Synthesis Parameters of Boehmite Sols with Different Particle Size

Sample	Hydrolysis time(h)	Molar ratio of H^+/Alkoxide	Average median particle size (nm)
BS40	3	0.15	40
BS200	24	0.07	200
BS630	24	0.04	630

2.2.2. Preparation of intermediate γ-alumina multilayer

A thin and defect-free γ-alumina multilayer was prepared on a macroporous α-alumina support by dipping-calcining with a series of dilute dipping solutions containing boehmite sols of different particle sizes. A commercial alumina membrane tube (PALL Corporation, Membralox® TI-70-25Z Membrane Tube, I.D.=7 mm, O.D.=10 mm) with a nominal pore size of 100 nm was used as the support. The preparation involved several steps. First, the alumina tube was cut to a length of 3-4 cm with a diamond saw and was connected to non-porous alumina tubes at both ends with ceramic joints. The ceramic joints were made with a glaze (Duncan IN 1001) fired at 1153 K for 0.5 h. Second, dilute dipping solutions were prepared by mixing the boehmite sols described in the previous section with a polyvinyl alcohol (PVA, M.W. = 72,000) solution and diluting with distilled water to obtain a 0.15 M concentration of the sol and a 0.35 wt. % concentration of the PVA. Three dipping solutions DS40, DS200 and DS630 were obtained from the boehmite sols BS40, BS200 and BS630, respectively. Third, the alumina support was dipped into the dipping solution and was withdrawn after 10 seconds at a rate of 0.01 m s^{-1} using a motor-driven dip-coating machine. Fourth, the dip-coated alumina was dried in ambient air for 24 h, and then was heated to 923 K in air at a rate of 1 K min^{-1} and calcined at

923 K for 2 h. The dipping-calcining process was successively carried out five times using different dipping solutions containing boehmite sols in the order of decreasing sol particle size: DS630, DS630, DS200, DS40 and DS40.

2.2.3. Preparation of silica-alumina composite membranes

The alumina-silica composite membranes were prepared using the previously described γ-alumina multilayer as the substrate by the deposition of a thin silica-alumina layer by the chemical vapor deposition method. This process places a silica-alumina layer on the surface of the substrate by the thermal decomposition of tetraethylorthosilicate (TEOS, Aldrich, 98%) and aluminum-tri-sec-butoxide (ATSB, Aldrich, 97%) at high temperature. The setup is shown in Figure 2.1. The support covered with the γ-alumina multilayer was installed concentrically inside a piece of glass tubing of 14 mm inside diameter using machined Swagelok fittings with Teflon ferrules. After placing the assembly in an electric furnace and heating it to 873 K at a heating rate of 1 K min^{-1}, an argon gas flow was introduced on the outer shell side and a dilute argon gas flow was passed on the inner tube side. After 0.5 h a TEOS carrier gas flow was passed through one bubbler filled with TEOS at 296 K while a separate ATSB carrier gas flow was passed through another bubbler filled with ATSB at a higher temperature in the range of 357-369 K. The two carrier gases were then premixed with the dilute Ar flow prior to introduction to the inside of the support tube. The molar ratio of ATSB to TEOS was adjusted by carefully controlling the flow rates of the carrier gases and the temperature of ATSB. The deposition time was varied from 3 to 6 h. After the CVD process was finished, the assembly was purged with the balance gas and dilute gas flows for 0.5 h.

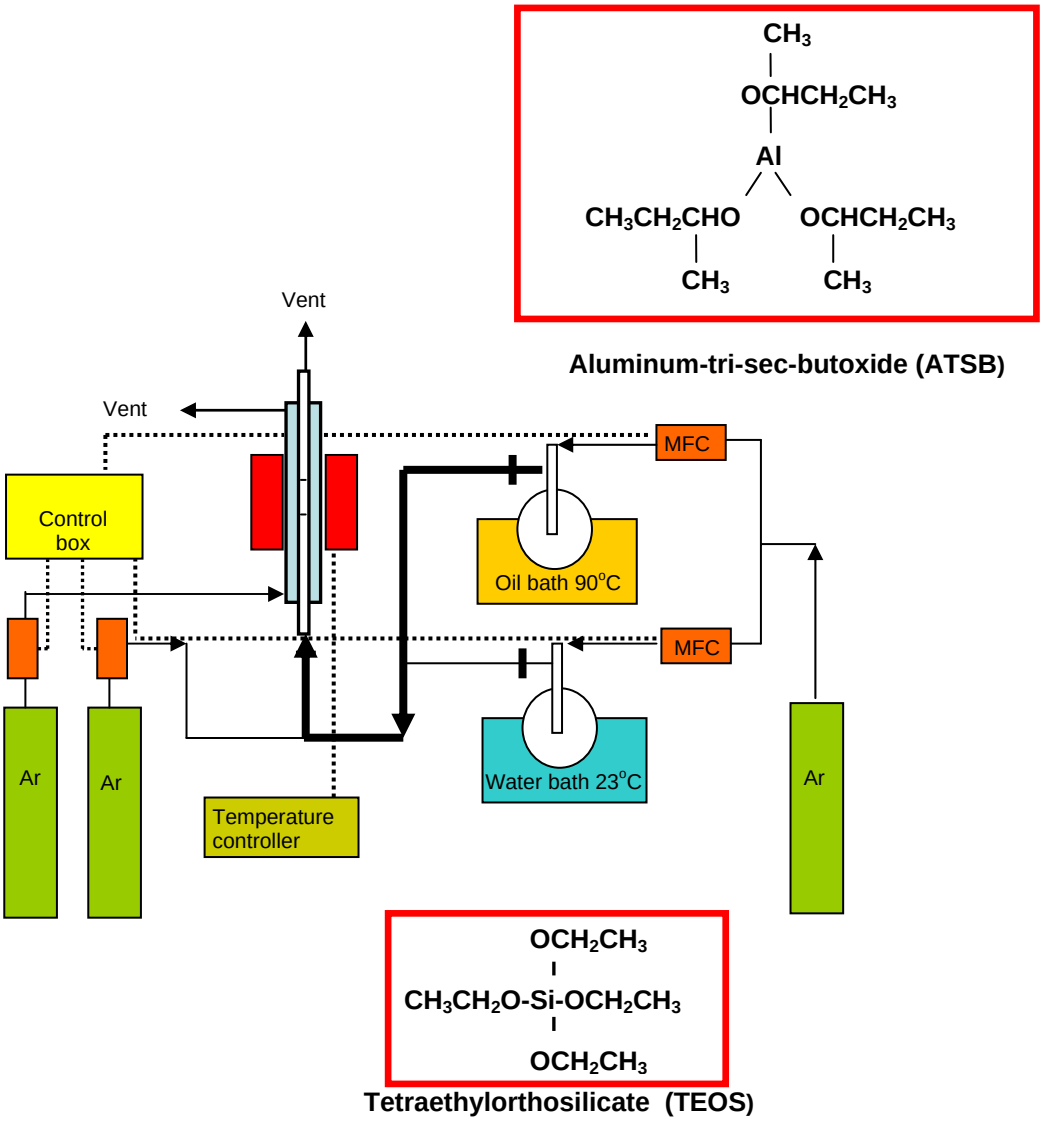

Figure 2.1. Schematic of dual-element CVD apparatus used in the deposition of the alumina-silica composite layer.

Table 2.2 lists the dual-element CVD process parameters. The composite membranes were labeled according to their composition. For example, the membrane 03AlSi was prepared with the use of a molar ratio of ATSB to TEOS of 0.03. In general, the TEOS concentration was fixed at 0.047 mol%, however, in two experiments with a molar ratio of ATSB to TEOS of 0.02,

lower TEOS concentrations of 0.032 and 0.022 mol% were employed. The resulting membranes were referred to as 02AlSi-L and 02AlSi-LL, respectively, indicating the lower TEOS concentrations.

Another related membrane was prepared using a commercial mesoporous alumina membrane tube as support with a nominal pore size of 5 nm (PALL Corporation, Membralox® TI-70-25G Membrane Tube, I.D.=7 mm, O.D.=10 mm). It was also cut into a length of 3-4 cm and then connected with non-porous alumina tubing at both ends by ceramic joints. Before CVD, the top surface of the support was modified with a thin layer of γ-alumina membrane by the dipping-calcining procedure using the dipping solution DS40.

2.2.4. Characterization

The concentration of the resulting boehmite sols was calculated from the volume of the sol and the known quantity of isopropoxide used. A dynamic light scattering analyzer (Horiba Model LB-500) was used to measure the particle size of the boehmite sols. The analyzer was calibrated using a standard polystyrene latex microsphere solution with mean diameter of 102 ± 3 nm (Duke Scientific Co.), and a value of 1.65 was used as the refractive index of boehmite for the internal calculation of particle size using a Fourier transform procedure.

Table 2.2. CVD Process parameters for the preparation of alumina-silica membranes (CVD temperature is always at 873 K)

Membrane	12AlSi	06AlSi	03Al-S	02AlSi	02AlSi-L	02AlSi-LL
TEOS Bath Temp. (K)	296	296	296	296	296	296
ATSB Bath Temp. (K)	377	369	363	358	357	357
TEOS Carrier Gas (μmol s^{-1})	3.7	3.6	3.7	3.7	3.3	3.3
ATSB Carrier Gas (μmol s^{-1})	6.11	5.7	4.0	4.2	4.1	4.1
Dilute Gas (μmol s^{-1})	7.3	7.7	9.2	9.2	15.5	25.4
Balance Gas (μmol s^{-1})	17.1	17.0	16.9	17.1	22.9	32.8
TEOS Concen. $\times 10^3$ (mol%)	47	47	47	47	32	22
ATSB Concen. $\times 10^3$ (mol%)	5.7	3.0	1.4	0.97	0.65	0.46
ATSB / TEOS (molar)	0.12	0.06	0.03	0.02	0.02	0.02

The cross-sectional microstructures of the intermediate layer of γ-alumina and the top layer of composite alumina-silica were obtained using a field emission scanning electron microscope (FESEM, Leo 1550). The samples were sputtered with gold before observation with

the electron microscope. The thickness of the top silica-alumina layer was obtained from cross-sectional photos with high resolution.

The gas permeation measurements were conducted at 873 K on H_2, CH_4, CO and CO_2 by admitting the pure gases at a pressure of around 202 kPa into the inner tube side, one end of which was closed, and measuring the quantity of gas flowing from the outer tube. The selectivity was calculated as the ratio of the permeances of H_2 to CH_4, CO and CO_2. Permeation of He, H_2, and Ne was measured in a similar manner at different temperatures in the range of 573-873 K.

The hydrothermal stability test was carried out at 873 K up to 520 h under an Ar flow containing 16 mol% or 57 mol% water vapor. First, an Ar flow at 15 μmol s^{-1} (flow rates in μmol s^{-1} can be converted to cm^3 (NTP) min^{-1} by multiplication by 1.5) was passed through a heated bubbler containing distilled water and was then introduced on the inner membrane tube side to directly contact the fresh composite membranes, while another Ar flow also at 15 μmol s^{-1} was maintained on the outer shell side. The Ar flow through the bubbler with temperatures of 329 K and 358 K gave an Ar stream with partial pressures of water vapor of 16.5 and 57.8 kPa, respectively, equivalent to 16 and 57 mol% water vapor. The H_2, CH_4 and CO_2 permeation rates were measured periodically during the hydrothermal stability test to monitor the changes in the permeance and selectivity. To make the measurements the water vapor was shut off for about 0.3 h to dry the membranes under a dry Ar flow. The wet Ar flow was resumed immediately after the permeance measurements.

2.3. Results and discussion

2.3.1. Morphology and structure of the composite membranes

Figure 2.2 (a)-(d) show the low and high resolution cross-sectional images of the mesoporous γ-alumina multilayer substrate and the alumina-silica composite membrane 02AlSi, which was prepared with the use of ATSB and TEOS concentrations of 9.7×10^{-4} and 4.7×10^{-2} mol %, respectively (molar ratio of ATSB/TEOS = 0.02). The γ-alumina multilayer substrate, which was prepared by sequentially placing coatings of boehmite sols of different particle sizes on a macroporous α-alumina support, had a 3-layer structure with different features, as shown in Figure 2.2(a). The thickness was around 1300 nm. The use of the dipping solution containing larger sol particles first resulted in no infiltration of γ-alumina particles into the pores (100 nm) of the macroporous support, indicating the success of the synthesis strategy [1]. After 4.5 h of dual-element CVD at 873 K on the alumina multilayer substrate, a thin and dense layer of alumina-silica was formed on the top of the multilayer substrate, as observed in Figure 2.2(b) and (d). The thickness of the composite top layer was measured from the high resolution image (Figure 2.2 (d)) to be 30-40.

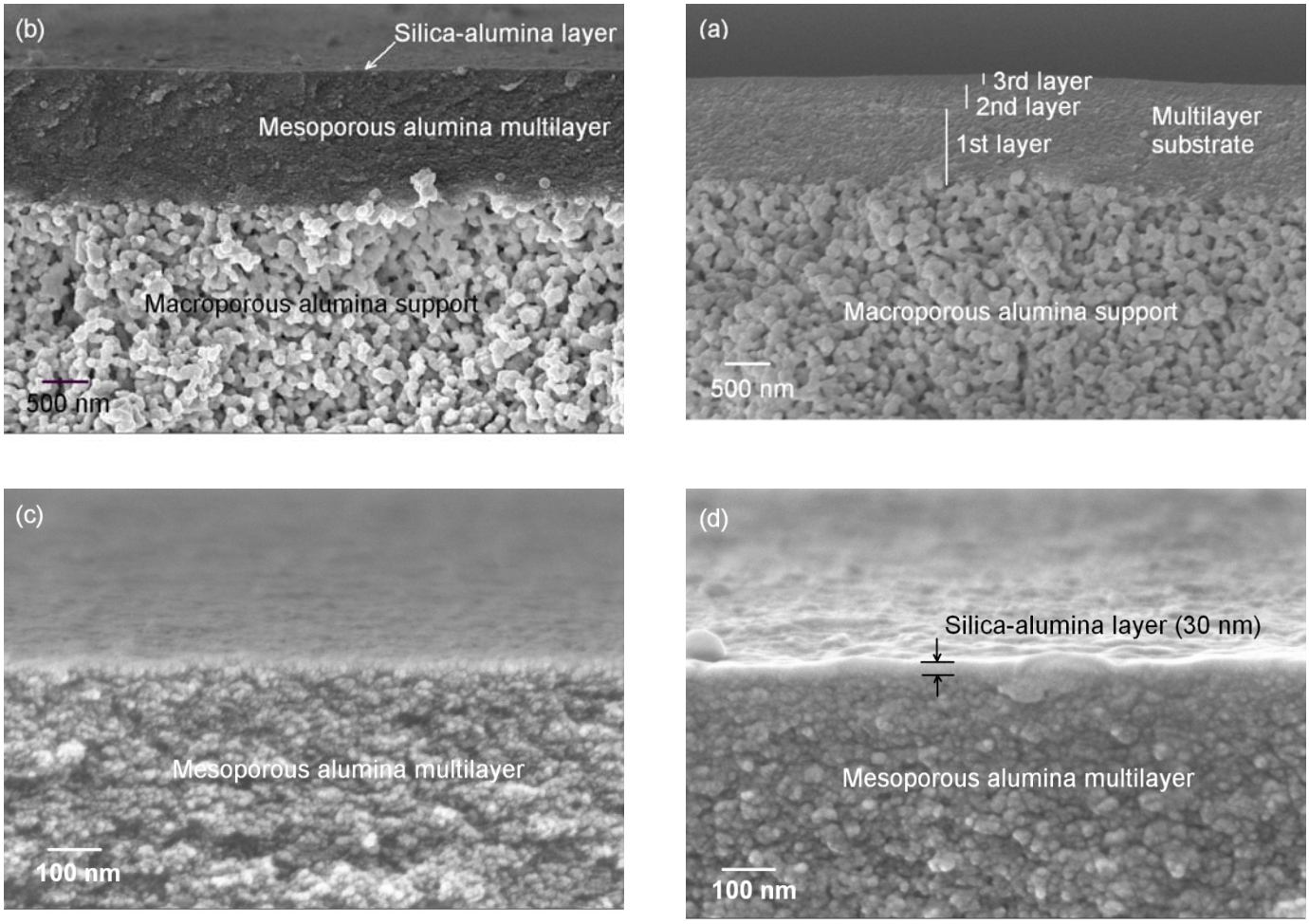

Figure 2.2. Scanning electron micrographs of fractured sections of graded γ-alumina multilayer substrate and composite alumina-silica membrane; Low resolution ×20,000 of substrate (a) and composite membrane (b); High Resolution ×100,000 of substrate (c) and composite membrane (d) (photograph by author)

2.3.2. Gas permeation properties of composite membranes

Figure 2.3 shows the changes with deposition time of the gas permeance and selectivity of the alumina-silica composite membrane 02AlSi at 873 K, which was prepared with the use of a molar ratio of ATSB/TEOS of 0.02. Before CVD, the freshly prepared γ-alumina multilayer substrate had high gas permeance to H_2, CH_4, CO and CO_2 of the order of 10^{-5} mol m^{-2} s^{-1} Pa^{-1} but rather low selectivity of H_2 over other gases. As the CVD deposition proceeded, the permeance of H_2 decreased more slowly than that of the other gases (CH_4, CO and CO_2) especially after 3 h of deposition, leading to an increase in the H_2 selectivity. After 4.5 h of deposition, the H_2 permeance decreased slightly to 1.6×10^{-7} mol m^{-2} s^{-1} Pa^{-1} at 873 K with the selectivity of H_2 over CH_4, CO and CO_2 being 940, 700 and 590, respectively. This corresponds to a H_2 purity above 99.8%.

Before CVD, the order of permeance of the gases, $H_2 > CH_4 > CO > CO_2$, followed the inverse square root of their molecular weight, as expected for Knudsen diffusion. The selectivities of H_2 over CH_4, CO and CO_2 were 2.8, 3.8 and 4.7, respectively, in good agreement with the values of 2.8, 3.7, and 4.7 predicted by Knudsen diffusion. This result is consistent with the pore size (3.7 nm) of the top layer of the γ-alumina multilayer substrate, which falls within the Knudsen diffusion regime. After 3 h of deposition, the gas permeance dropped to the order of 10^{-7} mol m^{-2} s^{-1} Pa^{-1} for H_2 and 10^{-8}-10^{-9} mol m^{-2} s^{-1} Pa^{-1} for CH_4, CO and CO_2, resulting in a selectivity of 20-100. It is likely that a continuous silica-alumina layer was completely formed at that point but that some defects or uncovered pores remained through which CH_4, CO and CO_2 could pass through. As the CVD deposition continued, these defects and pores were repaired

and, the permeance to CH_4, CO and CO_2 continued to drop fast while the permeance to H_2 was almost unchanged. As a result, the H_2 selectivity continued to increase quickly to 600-1000 after 4.5 h of deposition. The order of permeance of CO_2 > CO > CH_4 was in the order of the molecular size (CO_2 = 0.33 nm, CO = 0.376 nm, CH_4 = 0.38 nm [2]), indicating that the few remaining defects or uncovered pores fall in the size range of molecular sieves.

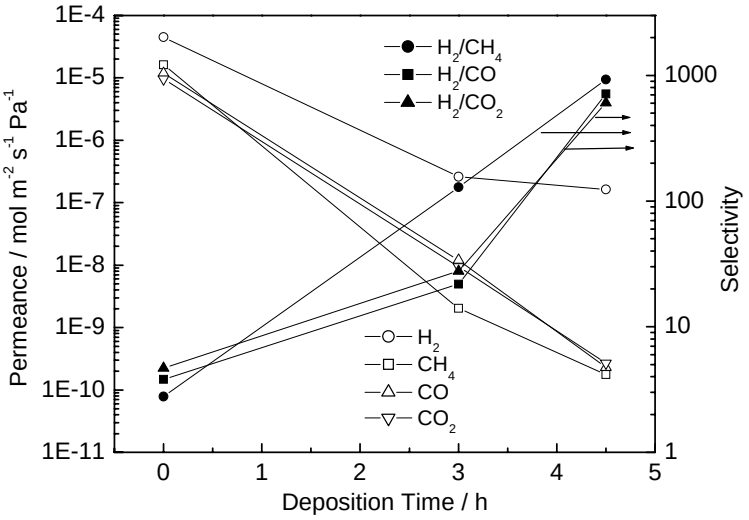

Figure 2.3. Changes of gas permeance and selectivity with deposition time of the alumina-silica composite membrane 02AlSi prepared at 873 K using the molar ratio of ATSB/TEOS of 0.02 and TEOS Concentration of 0.047 mol m^{-3}.

Figure 2.4 shows the changes of the gas permeance and selectivity on the alumina-silica composite membrane 03AlSi at 873 K with the deposition time. The membrane 03AlSi was prepared on the γ-alumina multilayer substrate by using dual-element CVD with the same TEOS concentration of 0.047 mol% as before but a higher molar ratio of ATSB/TEOS of 0.03, compared with the membrane 02AlSi. With the CVD deposition proceeding, the permeation

properties of the 03AlSi membrane showed the same trends as the 02AlSi membrane with a decrease in permeance and increase in selectivity with time as shown in Figure 2.3. However, the selectivity of the membrane 03AlSi improved much more slowly than that of 02AlSi, especially during the first 3 h. After 3h of CVD, the selectivity of H_2 over CH_4 and CO_2 of the former increased very little. When the CVD proceeded for another 3 h, the H_2 permeance started to decrease slowly, thus leading to a quick jump of the H_2 selectivity to around 200, but still lower than the case of the membrane 02AlSi. This behavior implied that higher molar ratios of ATSB/TEOS were not good for obtaining high-selectivity composite membranes.

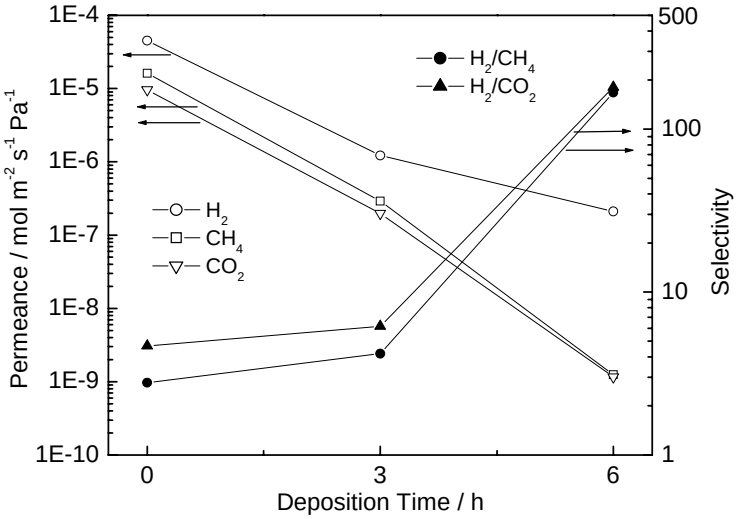

Figure 2.4. Changes of gas permeance and selectivity on the alumina-silica composite membrane 03AlSi at 873 K with the deposition time. The membrane was prepared using the molar ratio of ATSB/TEOS of 0.03 and TEOS concentration of 0.047 mol m^{-3}.

To confirm this finding, another two alumina-silica composite membranes were prepared using higher molar ratios of ATSB/TEOS (0.06 and 0.12). The results in Figure 2.5 clearly show

that the selectivity of H_2 over CH_4 decreased with increasing molar ratio of ATSB/TEOS, while the H_2 permeance increased. This is probably related to the faster deposition process when a higher molar ratio of ATSB/TEOS was used. Ha et al. [3] found that the deposition rate of the alumina-silica layer was much faster than that of the pure silica layer. The reason was probably that ATSB might act as a catalyst for the decomposition of TEOS and thereby accelerate the deposition rate of silica. Eversteijn [4] also reported that the presence of triisobutyl aluminium could cause the accelerated deposition of TEOS.

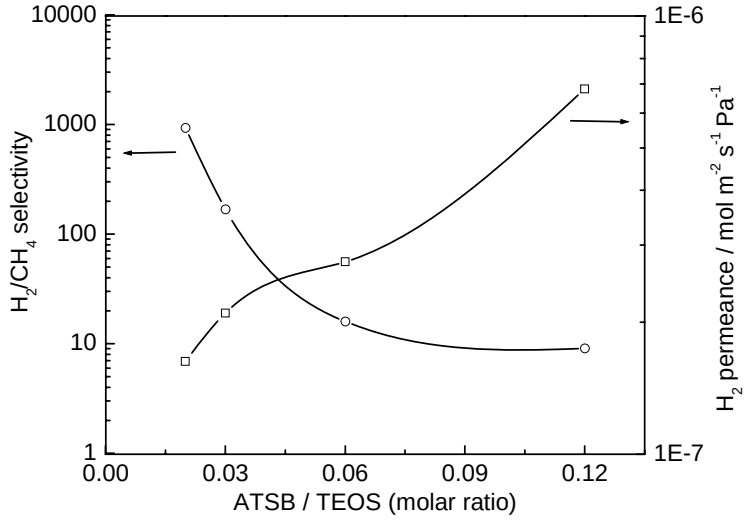

Figure 2.5. Permeation properties of the alumina-silica composite membranes prepared with the use of different molar ratio of ATSB/TEOS in the range of 0.02-0.12.

As described above, a TEOS concentration of 0.047 mol% was employed in this work. This concentration was much lower than that in previous reports on CVD derived silica membranes [3, 4, 5, 6, 7, 8, 9]. The low TEOS concentration gave rise to the thin membrane of around 40 nm shown in Fig. 2 with high gas permeability in the order of 10^{-7} mol m^{-2} s^{-1} Pa^{-1}. Ha et al. obtain a silica-alumina membrane with a thickness of 130 nm using a TEOS

concentration of 6.5 mol% [3]. Morooka et al. prepared silica membranes in macropores of alumina support by thermal decomposition of 0.29 mol% TEOS. They obtained a 150 nm thick membrane displaying a H_2 permeance of the order of 10^{-8} mol m^{-2} s^{-1} Pa^{-1}[5]. Tsapatsis and Gavalas carried out deposition of SiO_2 by passing the reactants $SiCl_4$ and H_2O at concentrations of 1-13 %. They obtained a 500 nm thick region of SiO_2 deposited in a porous Vycor tube which had low permeance [6]. However, too low a TEOS concentration probably poses the risk of leaving parts of the porous support uncovered producing defects, which in turn leads to low selectivity. Figure 2.6 shows the permeation properties of the composite membranes prepared with different TEOS concentrations in the range of 0.022-0.047 mol% (0.008-0.020 mol m^{-3}) but a fixed molar ratio of ATSB/TEOS of 0.02. It was found that when the TEOS concentration was lower than 0.03 mol m^{-3}, the obtained membrane showed much lower H_2 selectivity in the range of 10-20.

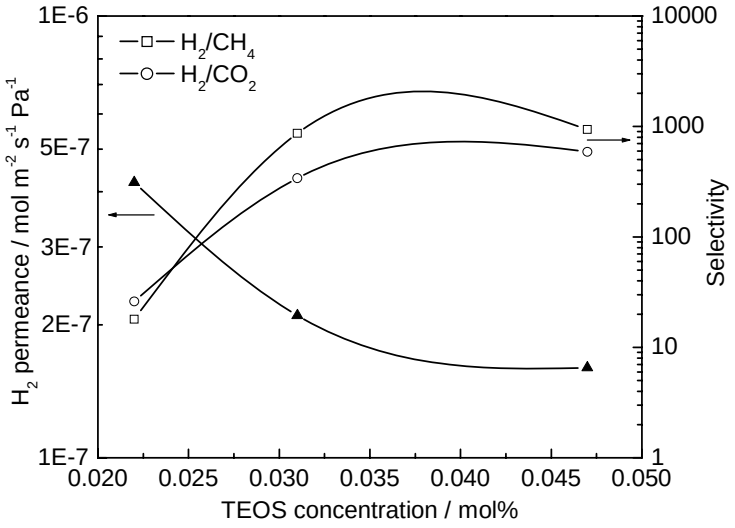

Figure 2.6. Permeation properties of the alumina-silica composite membranes prepared with different TEOS concentrations

Table 2.3 compares the permeation properties of the alumina-silica composite membranes prepared on different substrates by using the same CVD synthesis conditions. When the composite alumina-silica membrane was deposited on a graded 3-layer γ-alumina multilayer supported on a commercial 100 nm-pore size α-alumina tube, the H_2 selectivity was doubled or tripled while the H_2 permeance was increased by 60% compared to an ungraded 5 nm-pore size γ-alumina support. This is because the graded multilayer substrate has a finer and more uniform microstructure, that gave rise to a topmost layer with few defects.

Table 2.3. Effect of substrate on permeation properties of the alumina-silica membranes

Substrate		5 nm-pore size commercial γ-alumina	Graded 3-layer γ-alumina supported on 100 nm-pore size α-alumina
H_2 permeance (mol m^{-2} s^{-1} Pa^{-1})		1×10^{-7}	1.6×10^{-7}
H_2 selectivity	H_2/CH_4	430	940
	H_2/CO_2	170	590

2.3.3. Permeation mechanism through alumina-silica composite membranes

Figure 2.7 shows the dependence of the permeability of He, H_2, Ne, CO_2, CO, and CH_4 on the gas molecule kinetic diameter for the composite alumina-silica membrane 02AlSi at 873 K. The kinetic diameters of the molecules were obtained from the literature [2]. It was found that the permeance of He, H_2, and Ne, which have a small size was high, of the order of 10^{-8}-10^{-7}

mol m^{-2} s^{-1} Pa^{-1} while those of CO_2, CO, and CH_4 with larger molecular size was very low, of the order of 10^{-10} mol m^{-2} s^{-1} Pa^{-1}. It appears that a critical dimension that governs permeability is around 0.3 nm. Below this value species permeate rapidly, and above this value they do so with difficulty.

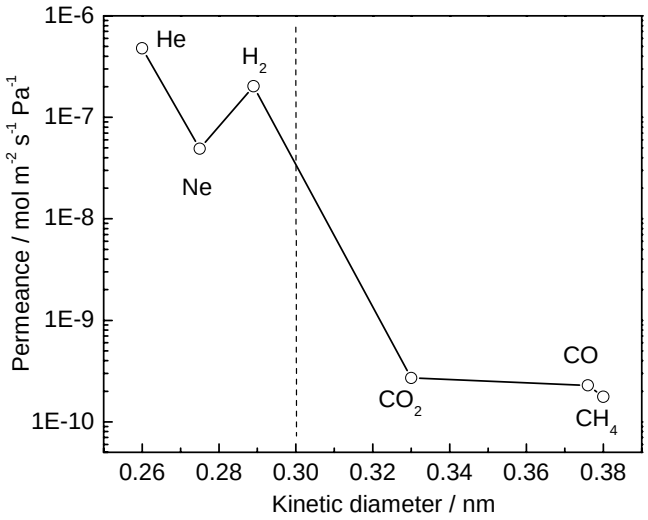

Figure 2.7. Permeance of gases with different molecule size through the composite membrane 02AlSi at 873 K prepared with the molar ratio of ATSB/TEOS of 0.02.

Figure 2.7 also shows an unexpected result, namely that the order of permeance of species with molecular size smaller than 0.3 nm is He > H_2 > Ne, which is unusual since it does not follow the size (He = 0.26 nm, H_2 = 0.289 nm, Ne = 0.275 nm [2]) nor the mass of the species (He = 4.0 au, H_2 = 2.01 au, Ne = 20.1 au). The same unusual order of permeance was found in a pure silica membrane as described in our previous report [10].

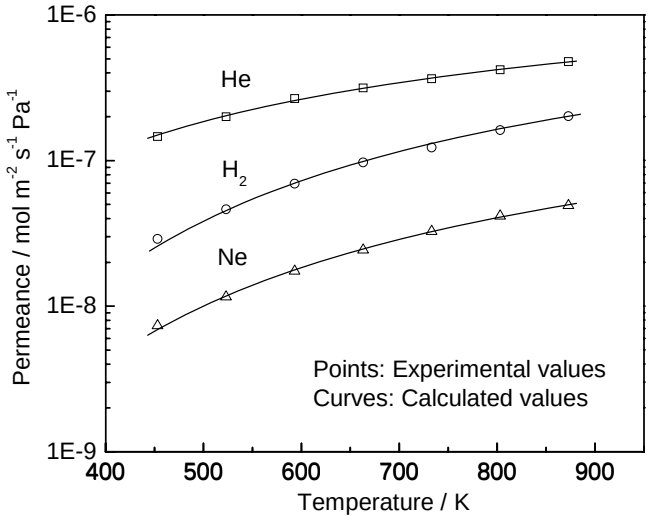

Figure 2.8. Permeance of He, H_2, and Ne at different temperature through the composite membrane 02AlSi at 873 K prepared with the molar ratio of ATSB/TEOS of 0.02.

Figure 2.8 shows the temperature dependence of the permeance of He, H_2 and Ne through this composite membrane. The permeance increased with temperature, indicating an activated diffusion transport mechanism through the membrane for these small gases. This unusual result can be quantitatively explained by a theory based on a mechanism involving jumps between solubility sites. Basically, the permeating species reside in solubility sites and jump randomly from site to site through passageways between the sites. The solubility sites in the composite membrane have a size of around 0.3 nm, which can explain the exclusion of CO_2 (0.33 nm), CO (0.376 nm) and CH_4 (0.38 nm) whose kinetic diameters are larger than the solubility sites. An equation was derived using statistical mechanics.

$$P = \frac{1}{6L}\left(\frac{d^2}{h}\right)\left(\frac{h^2}{2\pi mkT}\right)^{\frac{3}{2}}\left(\frac{\sigma h^2}{8\pi^2 IkT}\right)^{\alpha}\frac{(N_S/N_A)}{(e^{h\nu^*/2kT}-e^{-h\nu^*/2kT})^2}\,e^{-\Delta E_K/RT} \quad (2.1)$$

In this equation P is the permeance of the gas, L the thickness of the membrane, d the jump distance, m the mass of the species, h Planck's constant, k Boltzmann's constant, σ the symmetry factor of the species with σ = 2 in the case of H_2, I the moment of inertia, α an exponent accounting for incomplete loss of rotation with α = 0 for He and Ne and an optimal value of α = 0.2 for H_2 indicating a substantial loss of rotation, ν* the vibrational frequency of the species in the passageways between the sorption sites, T temperature, N_S the number of solubility sites available per m^3 of glass volume, N_A Avogadro's number, R the gas constant, and ΔE_K the activation energy for hopping between sorption sites. The calculated curves using this equation fit the experimental points very well, as shown as in Figure 2.8. The membrane thickness was taken to be *L* = 30 nm. Using a polynomial relationship previously found between d and N_S as shown in Equation (2) [10], the fitted parameters are summarized in Table 2.4.

$$d\ (nm) = a + bN_S + cN_S^2 + dN_S^3 \qquad (2.2)$$

where a = 0.84649, b = -1.74523×10^{-29}, c = 5.60055×10^{-58}, and d = -7.66678×10^{-87}. It can be seen that the calculated parameters are quite reasonable. The number of solubility site N_S is largest for He because of its small size compared with H_2 and Ne. The large N_S and low activation energy give rise to its high permeance, 2.5 and 10 times higher than that of H_2 and Ne, respectively. On the other hand, the vibrational frequency *v** is smallest for Ne due to its large weight compared with He and H_2, and accounts for the lowest permeance for Ne. The calculated jump distances are of the order of 0.8 nm, which indicates a passageway about 0.5 nm long between sites, considering the diameter of the solubility size of 0.3 nm.

Table 2.4. Calculated parameters for alumina-silica composite membrane

Gases	Kinetic Diameter (nm)	Weight (au)	N_s (sites m^{-3})	ν^* (s^{-1})	E_a (kJ mol^{-1})	d (nm)	Sum of least squares $\Sigma(Q_{calc.}-Q_{expl.})^2$
He	0.26	4	8.85×10^{26}	8.02×10^{12}	6.16	0.8315	1.16×10^{-16}
H_2	0.289	2	6.05×10^{26}	8.35×10^{12}	14.2	0.8361	6.16×10^{-17}
Ne	0.275	20	7.28×10^{26}	4.27×10^{12}	12.8	0.8341	1.55×10^{-18}

Table 2.5 compares the parameters for the composite alumina-silica membrane, pure silica membrane [11] and fused silica glass [12, 13, 14, 15, 16, 17, 18]. The number of solubility sites for the alumina-silica membrane (8.85×10^{26}, 6.05×10^{26} and 7.28×10^{26} m^{-3} for He, H_2 and Ne) is higher than that for the pure silica membrane (6.2×10^{26}, 3.8×10^{26} and 4.3×10^{26} m^{-3} for He, H_2 and Ne [11]), but lower than that for vitreous glass (2.3×10^{27}, 1.07×10^{27} and 1.3×10^{27} m^{-3} for He, H_2 and Ne [12, 13]). This implies that the addition of alumina makes the silica structure more restrictive, although the structure of the composite is much more open than vitreous silica glass. The calculated vibrational frequency ν^* values in the passageways were 8.02×10^{12} , 8.35×10^{12} and 4.27×10^{12} s^{-1} for He, H_2, and Ne, respectively, which are close to the values reported for a pure silica membrane [11] and silica glass [14]. The activation energies for permeation through the alumina-silica membrane are higher than through pure silica membranes, implying that the composite membrane has a more restrictive structure. On the other hand, the activation energies for permeation through the membranes (4.2-14.2 kJ mol^{-1}) are considerably smaller than through glass, which have values of 17.8-21.1 kJ mol^{-1} for He [15, 16]

and 37.2-38.3 kJ mol^{-1} for H_2 [17, 18], indicating that the structure of the silica-based membranes is different from that of silica glass, probably less dense and more open with larger Si-O ring structures through which the permeate must pass [10].

Table 2.5. Parameters for Pure Silica and Alumina-Silica Membranes and Silica Glass

Parameters	Gases	Pure Silica Membrane	Alumina Silica Membrane	Silica Glass
N_s (m^{-3})	He	6.2×10^{26}	8.85×10^{26}	2.3×10^{27}
	H_2	3.8×10^{26}	6.05×10^{26}	1.07×10^{27}
	Ne	4.3×10^{26}	7.28×10^{26}	1.3×10^{27}
ν^* (s^{-1})	He	7.0×10^{12}	8.02×10^{12}	6.90×10^{12}
	H_2	7.3×10^{12}	8.35×10^{12}	1.22×10^{12}
	Ne	3.5×10^{12}	4.27×10^{12}	4.38×10^{12}
E_a (kJ mol^{-1})	He	4.0	6.16	17.8-21.1
	H_2	10.4	14.2	37.2-38.3
	Ne	8.7	12.8	-

2.3.4. Hydrothermal stability of composite membranes

Figure 2.9 shows the change in H_2 permeance of the pure silica and composite alumina-silica membranes prepared using different molar ratios of ATSB/TEOS during the exposure to 16 mol % water vapor at 873 K for 130 h. It was found that although all the membranes suffered a lowering of their permeance during the first 10 h, the composite membranes clearly showed a

stronger resistance to water vapor than the pure silica membrane. After 50 h of exposure to water vapor, the H_2 permeance of the composite membranes stabilized, while the permeance through the silica membrane still kept declining. It is clear that the composite membranes prepared with increasing molar ratio of ATSB/TEOS showed better hydrothermal stability. The higher the content of alumina, the stronger the resistance to water vapor.

Figure 2.10 compares the long-term hydrothermal stability between the pure silica membrane and the composite membrane 03AlSi obtained with the molar ratio of ATSB/TEOS of 0.03. After exposure to 16 mol% water vapor at 873 K for 520 h, the H_2 permeance through the composite membrane was decreased by less than half, while the H_2 permeance through the pure silica membrane was reduced by more than 15 times, attaining a value of less than 10% of the original value. The composite membrane 03AlSi was further exposed to a higher humidity environment containing 60 mol % water vapor at 873 K for another 135 h and the decrease in H_2 permeance was found to be less than 5%. Clearly, the introduction of alumina significantly improves the hydrothermal stability of the silica membranes.

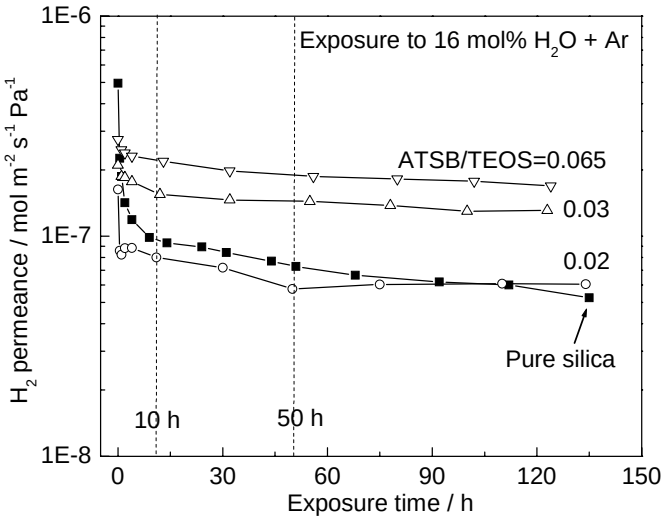

Figure 2.9. Changes in H_2 permeance through the pure silica and composite alumina-silica membranes prepared using different molar ratios of ATSB/TEOS during the exposure to 16 mol% water vapor for 130 h

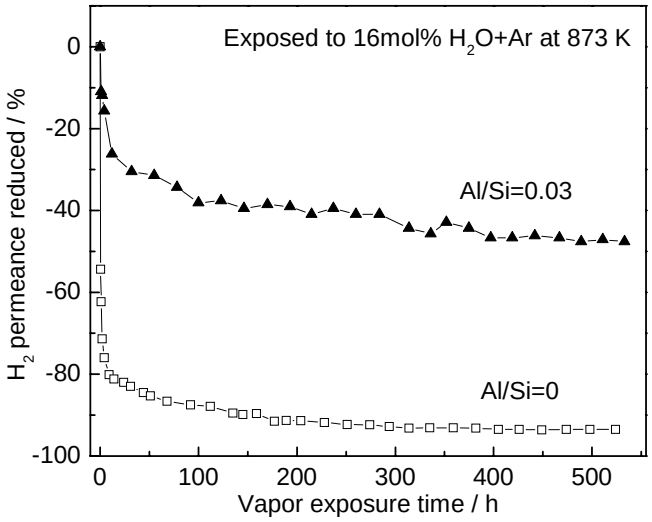

Figure 2.10. Long-term hydrothermal stability between the pure silica membrane and the composite membrane 03AlSi prepared using molar ratio of ATSB/TEOS of 0.03

2.4. Conclusions

A hydrothermally stable and hydrogen selective membrane composed of silica and alumina was successfully prepared on a macroporous alumina support by chemical vapor deposition in an inert atmosphere at high temperature. Before the deposition of the silica-alumina composite, multiple graded layers of alumina were coated on the alumina support with a mean pore size of 100 nm by the sequential application of three boehmite sols with gradually decreasing sol particle sizes of 630, 200 and 40 nm, respectively. The SEM microphotograph of the fracture surface of the composite membrane indicated a thin silica-alumina layer with a thickness of 30-40 nm deposited on the multilayer alumina substrate.

The resulting supported composite silica-alumina membrane had high permeability for hydrogen in the order of 10^{-7} mol m^{-2} s^{-1} Pa^{-1} at 873 K with a selectivity of H_2 over CH_4, CO and CO_2 of 940, 700 and 590, respectively. Significantly, the composite membrane exhibited much higher stability to water vapor at the high temperature of 873 K in comparison to pure silica membranes. After exposure to 16 mol% water vapor at 873 K for 520 h, the H_2 permeance through the composite membrane was decreased by less than half, while the H_2 permeance through the pure silica membrane was reduced by more than 15 times. The introduction of alumina into silica in the ratios of Al:Si of 0.02 to 0.065 makes the silica structure more stable and slows down the silica densification process.

In addition, the same unusual permeance order of He> H_2> Ne previously observed for the pure silica membrane was also observed for the alumina-silica membrane, indicating that the

silica structure did not change much after introduction of the alumina. A higher number of solubility sites and a higher activation energy implies that the composite membrane is more dense than the pure silica membranes.

References

[1] Y. Gu, S.T. Oyama, To be submitted to J. Membr. Sci.

[2] D.W. Breck, Zeolite Molecular Sieves: Structure, Chemistry and Use, Wiley, New York, 1974, p.636

[3] H. Y. Ha, J. S. Lee, S. W. Nam, I.W. Kim, S.-A. Hong, J. Mater. Sci. Lett. 16 (1997) 1023-1026

[4] F.C. Eversteijn, Philips Res. Rep. 21 (1966) 379-386

[5] S. Morooka, S. Yan, K. Kusakabe, Y. Akiyama, J. Membr. Sci. 101 (1995) 89-98

[6] M. Tsapatsis, G. Gavalas, J. Membr. Sci. 87 (1994) 281-296

[7] H.Y. Ha, S.W. Nam, S.-A. Hong, W.K. Lee, J. Membr. Sci. 85 (1993) 279-290

[8] H.Y. Ha, J.S. Lee, S.W. Nam, I.W. Kim, S.A. Hong, J. Mater. Sci. Lett. 16 (1997) 1023-1026

[9] S.-I. Nakao, T. Suzuki, T. Sugawara, T. Tsuru, S. Kimura, 37 (2000) 145-152

[10] S. T. Oyama , D. Lee, P. Hacarlioglu, R. F. Saraf, J. Membr. Sci. 244 (2004) 45-53

[11] S.T. Oyama, Y. Gu, To be submitted to Nature, Materials

[12] J.E. Shelby, J. Appl. Phys., 47 (1976) 135

[13] J.E. Shelby, J. Appl. Phys., 48 (1977) 33875

[14] J.F. Shackelford, P.L. Studt, R.M. Fulrath, J. Applied Phys. 43 (1972) 1619-1626

[15] R.W. Lee, R.C. Frank, D.W. Swets, J. Chem. Phys. 36 (1962) 1062

[16] R.W. Lee, J. Chem. Phys. 38 (1963) 448

[17] J.E. Shelby, J. Am. Ceram. Soc. 55 (1972) 61-64

[18] J.E. Shelby, J. Am. Ceram. Soc. 54 (1971) 125-126